

Enhanced Detection of Geomorphic Changes in the Khor Al-Sabiyeh Coastal Environment Using SAR, Optical Imagery, and Machine Learning

Aldousari A.E.^{1*}, Oyedotun T.D.T.², AlKhaled S.R.³ and Burningham H.⁴

¹Department of Geography, Kuwait University, Kuwait City, Kuwait

²Department of Geography, Faculty of Earth and Environmental Sciences (FEES),
University of Guyana, P O Box 10 1110, Turkeyen Campus, Guyana

³Department of Architecture, Kuwait University, Kuwait City, Kuwait,
P.O. Box 5969, Safat 13030, Kuwait

³Coastal and Estuarine Research Unit, UCL Department of Geography,
Gower Street, London, WC1E 6BT

[*dr.dousari@ku.edu.kw](mailto:dr.dousari@ku.edu.kw) (*Corresponding author)

Abstract Coastal wetlands are among the most ecologically significant landscapes, yet they are highly susceptible to geomorphic changes driven by both natural processes and anthropogenic pressures. This study presents an integrated remote sensing and machine learning approach to enhance the detection of geomorphic changes in Khor Al-Sabiyeh, a critical coastal wetland in Kuwait. By utilising the complementary strengths of Synthetic Aperture Radar (SAR) and optical imagery (Landsat-8 and Sentinel-2), we developed an analytical framework that overcomes the limitations of conventional monitoring methods. Using Google Earth Engine (GEE) for data preprocessing, we generated cloud-free annual composites for 2023 and computed a suite of spectral indices, including NDVI, NDMI, MNDWI, GCVI, SR, and custom band ratios, which provided detailed insights into geomorphic dynamics, water bodies, and land surface conditions. The results revealed distinct spatial patterns of erosion, accretion, and land cover changes, which have direct implications for environmental planning in the region. The results from this research show the potential of integrating SAR, optical datasets, and machine learning for a timely and accurate assessment of landscape changes in fragile coastal systems. The methodological framework adopted in this study is transferable and scalable, offering valuable applications for similar systems globally. This approach supports evidence-based environmental governance and enhances resilience in the face of climate change and human-induced alterations.

Keywords: Coastal Wetlands, Geomorphic Change Detection, Khor Al-Sabiyeh, Machine Learning, Optical Imagery, Remote Sensing Integration, Synthetic Aperture Radar (SAR).

Introduction

Coastal wetlands are among the most dynamic and ecologically vital ecosystems on Earth, providing essential ecological services such as flood regulation, shoreline stabilization, carbon sequestration, water purification, and serving as critical habitats for diverse species of flora and fauna (Mitsch & Gosselink, 2015). Their productivity and ecological functions are particularly important in arid and semi-arid regions, where they often represent rare ecological refuges. However, these ecosystems are inherently fragile, and their geomorphic stability is constantly

influenced by both natural processes and anthropogenic pressures. Understanding the spatial and temporal dynamics of these wetlands is therefore crucial for devising effective conservation and sustainable management strategies.

Geomorphic changes in coastal wetlands, such as erosion, accretion, sediment deposition, and landform alterations, are key indicators of ecosystem health and resilience. These changes are shaped by a complex interplay of hydrodynamic forces, sediment supply, vegetation cover, and human interventions (Adam et al., 2010). Rising sea levels, storm surges, and tidal influences often drive natural morphological adjustments, while urban expansion, industrial activities, dredging, and reclamation projects accelerate degradation. Accurate detection and monitoring of geomorphic changes are therefore essential for identifying ecosystem vulnerabilities, predicting future transformations, and supporting adaptive management policies (Murray et al., 2019).

Kuwait's coastal zone is characterised by a mosaic of tidal flats, salt marshes, and sabkhas, which are ecologically and geomorphologically unique within the Arabian Gulf. Among these, Khor Al-Sabiyeh represents a particularly significant coastal wetland system, functioning as a vital habitat for migratory birds, a nursery ground for marine organisms, and a buffer against coastal hazards (Al-Rashed et al., 2017; Al-Hurban et al., 2008). Its location along the northwestern Arabian Gulf exposes it to strong hydrodynamic forces and sedimentary processes, making it highly dynamic but also increasingly vulnerable. These wetlands also hold cultural and socio-economic value, given their proximity to development zones and their role in supporting biodiversity and fisheries.

Despite their importance, the Khor Al-Sabiyeh wetlands are under growing pressure from climate change and human activities. Projected sea-level rise threatens to inundate low-lying areas, while increasing salinity and temperature stress may alter vegetation composition and ecological functioning (Nicholls & Cazenave, 2010). Simultaneously, coastal development, oil-related industrial activities, and land reclamation projects have intensified geomorphic disturbances, leading to habitat fragmentation and loss (Al-Attar et al., 2023). Without systematic monitoring, these processes risk compromising the ecological integrity of the wetland, undermining both its biodiversity value and the ecosystem services it provides to surrounding communities.

Remote sensing has emerged as a powerful tool for monitoring geomorphic changes in coastal wetlands, enabling continuous observation across spatial and temporal scales that would be difficult to achieve through field surveys alone. Optical sensors, such as those onboard Landsat and Sentinel-2, provide valuable insights into vegetation distribution, sediment patterns, and surface water dynamics, supporting the detection of coastal change processes (Mandanici & Bitelli, 2016; Delegido et al., 2011). However, their effectiveness can be limited by atmospheric conditions, cloud cover, and spectral ambiguities in highly reflective sabkha and tidal flat environments. To address these limitations, radar-based systems, particularly Synthetic Aperture Radar (SAR), have become increasingly important for their ability to penetrate clouds and detect surface roughness, inundation, and moisture variations (Ban et al., 2015).

The integration of SAR and optical imagery offers significant advantages for characterising geomorphic processes in coastal systems. While optical data are particularly effective for mapping vegetation and sediment characteristics, SAR data provide complementary information on soil moisture, surface roughness, and inundation dynamics, especially in areas obscured by clouds or with high reflectivity (Müller et al., 2020; Zhang et al., 2021). By combining these datasets, researchers can obtain a more comprehensive representation of geomorphic conditions, thereby improving the accuracy of change detection and enhancing their ability to monitor subtle geomorphic transformations in complex coastal environments, such as Khor Al-Sabiyeh.

In recent years, advances in machine learning have further expanded the analytical potential of remote sensing for coastal geomorphic studies. Algorithms such as Random Forest (RF), Support Vector Machines (SVM), and deep learning models have proven effective in integrating multi-sensor datasets, reducing classification uncertainties, and improving the detection of land cover and geomorphic changes (Belgiu & Drăguţ, 2016; Ma et al., 2019). These approaches are particularly valuable in heterogeneous environments like Kuwait's coastal wetlands, where complex interactions between sediment, vegetation, and hydrodynamics challenge conventional image processing techniques. By combining machine learning with SAR-optical data fusion, researchers can move beyond traditional threshold-based methods to more robust, data-driven approaches for monitoring coastal change.

This study aims to enhance the detection of geomorphic changes in the coastal wetlands of Khor Al-Sabiyeh by integrating SAR and optical remote sensing data with machine learning techniques. Specifically, the objectives are: (1) to collect and preprocess SAR and optical imagery of Khor Al-Sabiyeh coastal wetlands; (2) to develop a machine learning model that integrates SAR and optical data for detecting geomorphic changes; and (3) to analyse the detected changes and assess their implications for conservation and management. By advancing methods for multi-sensor integration and automated change detection, this research contributes to a more comprehensive framework for understanding and managing fragile wetland ecosystems in arid coastal regions.

Methodology

a. Study Area:

Figure 1 presents cloud-free optical imagery of Kuwait for the year 2023, derived from different satellite platforms: (a) Landsat-7, (b) Landsat-8, (c) Sentinel-2, and (d) a composite integration of all three datasets. The imagery highlights spatial variability across Kuwait's terrestrial and coastal landscapes, offering insights into land cover, vegetation distribution, and environmental conditions. The colour-coded scale, ranging from green (low values) to red (high values), reflects the number of clear observations at the pixel level, a critical factor in reducing uncertainty for geomorphic and ecological monitoring.

Figure 1 (a), derived from Landsat-7, reveals a moderate distribution of usable observations, though with visible striping artefacts inherent to the Scan Line Corrector (SLC) failure that has affected the satellite since 2003. These data gaps underscore the limitations of relying solely on Landsat-7 for consistent coverage, although it remains valuable for long-term historical continuity. Figure 1 (b), from Landsat-8, provides improved clarity, spatial resolution, and radiometric sensitivity, reducing striping errors and offering more reliable spectral representation of Kuwait's arid terrain, vegetation patches, and coastal wetlands such as Khor Al-Sabiyeh. Figure 1 (c), based on Sentinel-2, shows higher density of valid observations due to the satellite's finer spatial resolution (10–20 m) and frequent revisit cycle (5 days at the equator). This enables sharper delineation of vegetation zones in northern Kuwait, urban expansion around Kuwait City, and agricultural patterns in the southern regions. The Sentinel-2 data contribute significantly to monitoring small-scale geomorphic and ecological processes, particularly in coastal and wetland ecosystems where

changes occur rapidly. Figure 1 (d), the combined composite of Landsat-7, Landsat-8, and Sentinel-2, maximises spatial and temporal coverage by integrating the strengths of all three platforms. This fusion reduces data gaps caused by cloud cover, sensor limitations, or acquisition frequency, resulting in a robust and spatially continuous dataset. The enhanced coverage improves the reliability of change detection, allowing more precise monitoring of land degradation, desertification, and urban encroachment in Kuwait. Furthermore, the integration supports more advanced machine learning applications, as the enriched dataset enhances the discriminatory power for classifying and detecting geomorphic changes across the landscape.

The analysis of cloud-free optical imagery over Kuwait underscores how sensor design and operational characteristics dictate the suitability of each platform for environmental and geomorphic monitoring. Landsat-7, though historically invaluable for long-term Earth observation, has been hampered since 2003 by the Scan Line Corrector (SLC) failure, producing data gaps and striping that complicate pixel-level time-series analysis and reduce effective spatial continuity (USGS, 2003). Despite this limitation, the multispectral configuration of Landsat-7 (visible, NIR, SWIR thermal bands) preserves its utility for historical baselines and trend analyses. Landsat-8 represents a substantive step forward: the Operational Land Imager (OLI) and the Thermal Infrared Sensor (TIRS) provide higher radiometric fidelity (12-bit quantization), improved signal-to-noise ratios, and refined spectral response functions, which together enhance the detection of subtle reflectance differences related to soil moisture, vegetation stress, and urban surface materials (Irons, Dwyer, & Barsi, 2012; Roy et al., 2014). These radiometric improvements make Landsat-8 more reliable for discriminating low-contrast surface features common in arid environments.

Sentinel-2 complements and extends the capabilities of the Landsat series by delivering finer spatial resolution and greater temporal frequency. With 10–20 m resolution in key optical bands and a nominal 5-day revisit period (with the twin-satellite constellation), Sentinel-2 excels at capturing rapid or small-scale changes in land cover and coastal morphology (Drusch et al., 2012). The inclusion of red-edge bands and additional narrow NIR/SWIR channels improves sensitivity to vegetation chlorophyll and stress—attributes particularly useful for mapping sparse halophytic vegetation and early successional stages on sabkhas and tidal flats (Delegido et al., 2011). Operationally, the complementary spectral and revisit characteristics of Sentinel-2 and Landsat (i.e., Sentinel-2's high spatial/temporal resolution

and Landsat's long historical archive and thermal information) argue for a fused, multi-sensor approach: fusion maximises data availability, mitigates platform-specific gaps (e.g., SLC-off artefacts on Landsat-7 or cloud contamination), and utilises the radiometric precision of Landsat-8 with Sentinel-2's spatial detail (Mandanici & Bitelli, 2016; Müller et al., 2020). Such synergy is particularly advantageous in arid coastal regions where high surface reflectance, rapid sediment dynamics, and ephemeral vegetative patches require both sensitive radiometry and fine spatial sampling for robust detection.

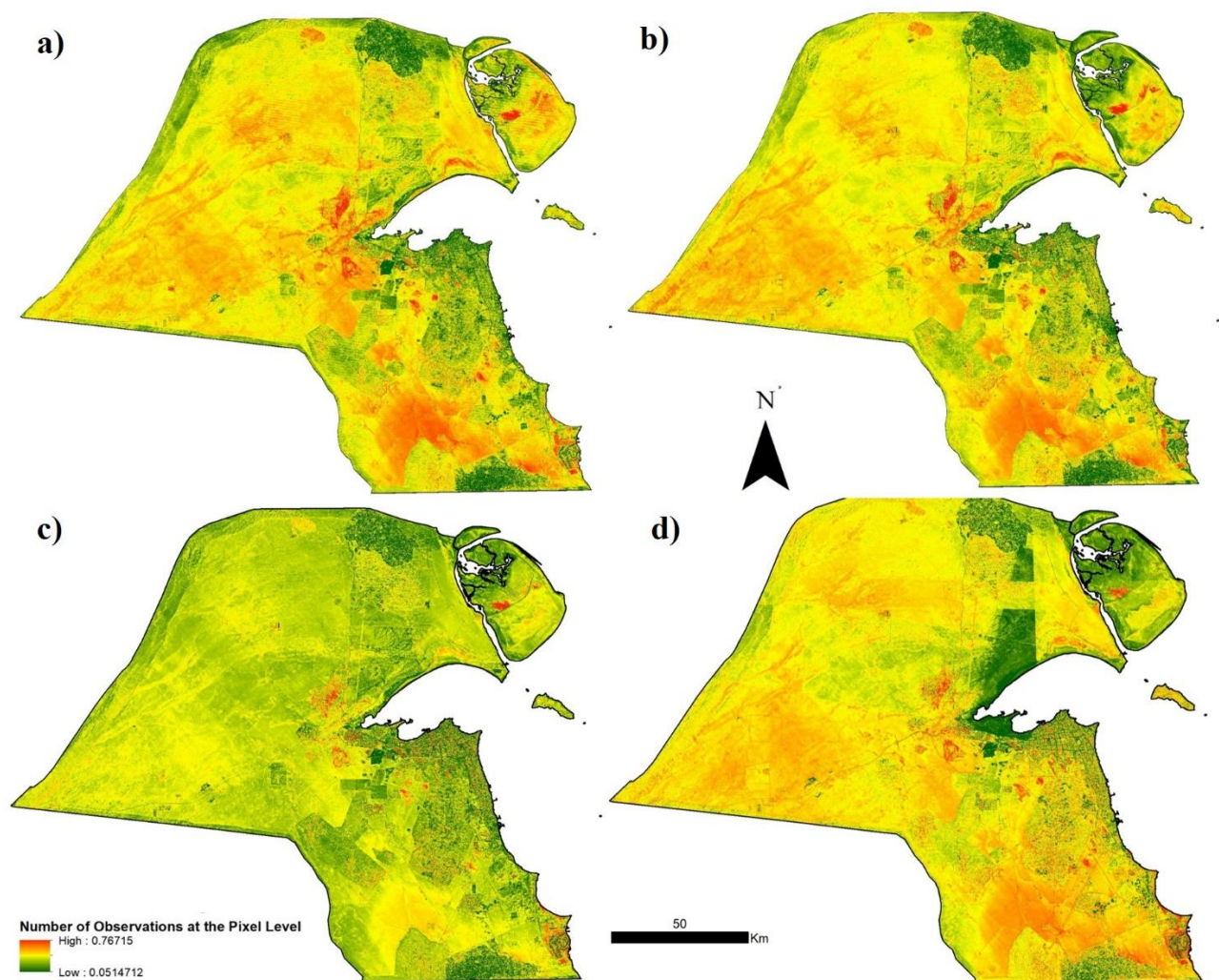


Figure 1: Cloud-free optical imagery (a) Landsat-7, (b) Landsat-8, (c) Sentinel-2 and (d) the combination of the three images, over Kuwait for the year 2023.

Khor Al-Sabiyeh (Figure 2b), located in Kuwait, is a vital coastal wetland characterised by its unique ecological features and vulnerability to both natural and anthropogenic influences. This area serves as an essential habitat for various species and plays a significant role in the regional ecological balance. Given the importance of Khor Al-Sabiyeh, this study

focuses on exploring the diverse remotely sensed images in monitoring geomorphic changes to better understand and manage these critical ecosystems.

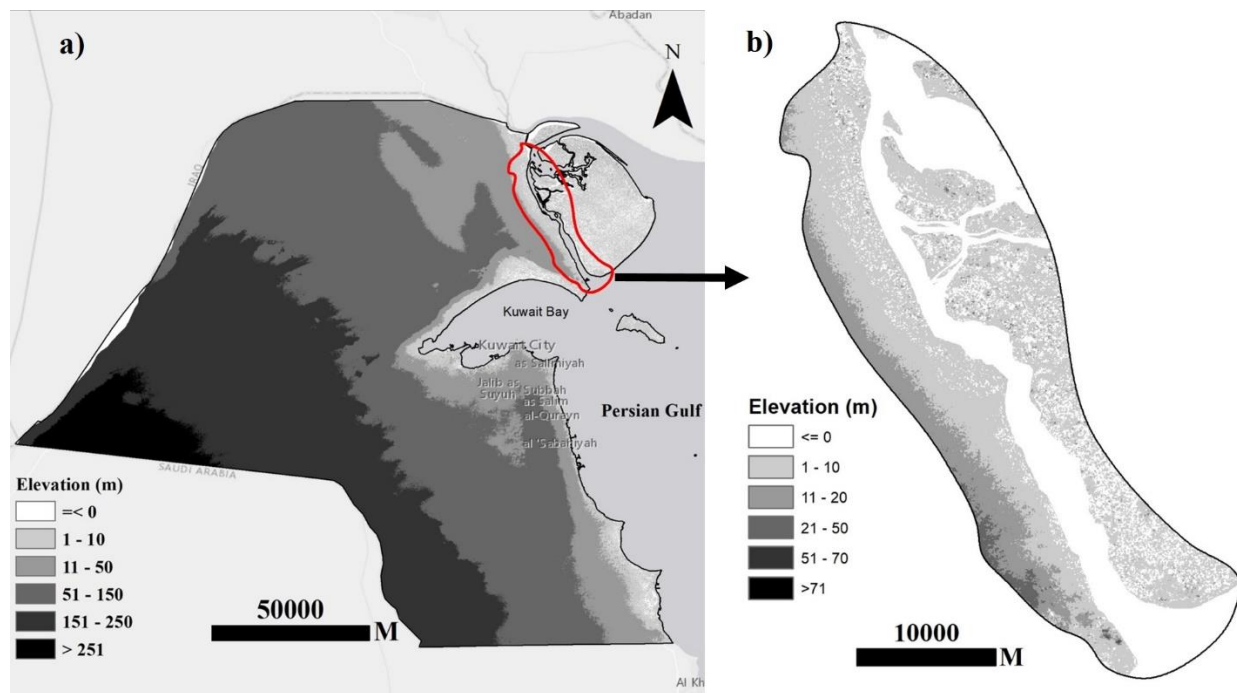


Figure 2: Map of Kuwait showing the country's elevation (a). Inset: Khor Al-Sabiye (b).

b. Data Acquisition and Preprocessing:

Data from the Landsat 7 ETM+, Landsat-8 Operational Land Imager (OLI) and Sentinel-2 MultiSpectral Instrument (MSI) were acquired through Google Earth Engine (GEE). GEE is a cloud-based analysis and visualisation platform that provides access to a vast catalogue of geospatial datasets, making it ideal for handling the large file sizes and processing demands associated with satellite imagery.

- Landsat 7 ETM+ imagery provided by the U.S. Geological Survey (USGS, 2023).
- Landsat-8: Collection 2 Tier 1 dataset, filtered to the year 2023 (USGS, 2023).
- Sentinel-2: Datasets filtered to the year 2023 (ESA, 2023).

In GEE, the Landsat-7, Landsat-8 and Sentinel-2 datasets were filtered to include images from the year 2023. A cloud mask was applied to each scene using the quality assessment bands, and annual composites were created using the median value of each pixel across the full year of imagery.

For Sentinel-2, the preprocessing steps included:

- Cloud Masking: Using the quality assessment bands to mask clouds and cloud shadows.

- Compositing: Creating annual composites by taking the median value of each pixel throughout the year 2023 to ensure a consistent and cloud-free dataset.

The final composite was re-projected to a 30 m spatial resolution for consistency across datasets.

c. Spectral Indices:

Multiple red-green-blue composites and standard spectral indices were created to serve as input variables for the machine-learning classification. These indices include:

- Normalised Difference Vegetation Index (NDVI): Measures vegetation greenness as a proxy for health (Rouse et al., 1974).
- Normalised Difference Moisture Index (NDMI): Quantifies vegetation with high water content (Gao, 1996).
- Modified Normalised Difference Water Index (MNDWI): Distinguishes open water features (Xu, 2006).

Additional indices included:

- Simple Ratio (SR): Quantifies vegetation density (Jordan, 1969).
- Band Ratio 54: Distinguishes water bodies from vegetation (Sabins, 1996).
- Band Ratio 35: Enhances urban areas and distinguishes water from vegetation (Chen et al., 2005).

These indices were selected based on their effectiveness in previous studies that mapped mangroves and other coastal vegetation types (Giri et al., 2011; Kuenzer et al., 2011).

Results and Discussion

(a) NDVI:

The Normalised Difference Vegetation Index (NDVI) is a widely used remote sensing metric that provides information about vegetation health and density. It is calculated from the visible and near-infrared light reflected by vegetation. Figure 3 presents the analyses of NDVI for values for the Khor Al-Sabiyeh, Kuwait. The NDVI values in the legend indicate:

- 1 to 0 (generally indicates water, clouds, snow, or barren areas with little to no vegetation);
- 0 to 0.2 (which represents bare soil, rocks, or very sparse vegetation);
- 0.2 to 0.5 (which indicates areas with low to moderate vegetation, such as shrubs, grasslands, or sparse forests);
- 0.5 to 0.8 (which suggests healthy, dense vegetation, typically seen in forests and

croplands), and 0.8 to 1 (which reflects very lush and dense vegetation, usually indicating rainforests or other highly vegetated regions). The interpretation of these suggests that:

- Lower Values, that is, low values near 0, generally indicate non-vegetated surfaces like rocks, bare soil, or water. These surfaces reflect more in the visible wavelengths and less in the near-infrared, resulting in lower NDVI values.
- Higher Values, that High NDVI values close to 1 are associated with healthy, photosynthetically active vegetation. This is because plants strongly absorb visible light for photosynthesis and reflect much of the near-infrared light.

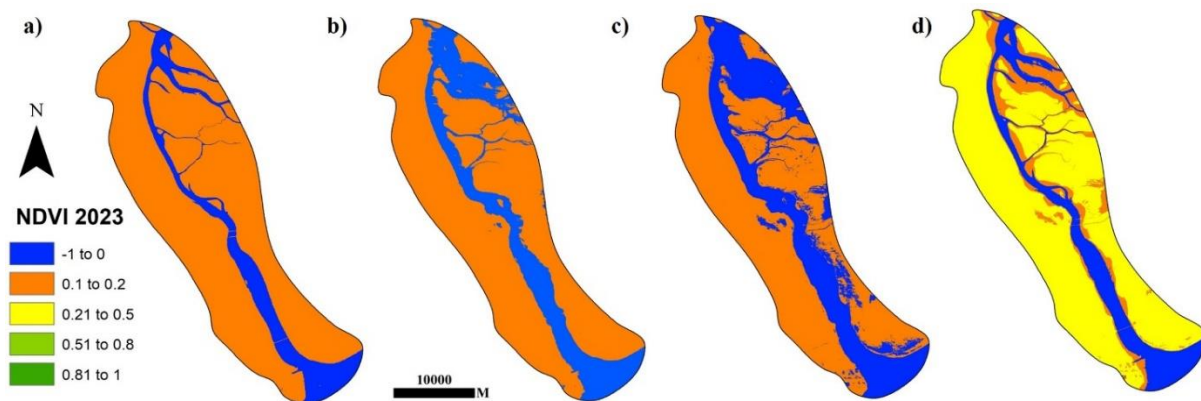


Figure 3: The NDVI for Khor Al-Sabiyeh, Kuwait (a) Landsat 8, Landsat 7 (b), Sentinel 2 (c) and the fusion of the three images (d).

Figure 3 shows NDVI derived from: (a) Landsat 8; (b) Landsat 7; (c) Sentinel-2, and (d) Fusion of all three datasets. Figure 3 (a) Landsat 8, dominated by orange tones (0.1–0.2), representing bare soil, sandy flats, or sparse vegetation. The coastal channels and tidal areas show blue (NDVI < 0), indicative of water bodies and saturated sediments. Some areas of low to moderate vegetation (0.21–0.5, yellow) are visible but not extensive. For Figure 3 (b), Landsat 7, the findings of the analysis show a similar distribution as Landsat 8, but with slightly less contrast. Vegetation patches are less distinct, and the spectral limitations of the older Landsat 7 sensor may underrepresent vegetation signals. This is still useful for identifying broad geomorphic zones such as mudflats and tidal inlets. Figure 3 (c) Sentinel-2, provides higher spatial detail and more accurately delineates vegetation patches along tidal creeks and marshes. The finer resolution improves detection of geomorphic transitions, such as between mudflats and vegetated sabkhas; and, captures narrow bands of vegetation growth better than Landsat imagery. Figure 3 (d), Fusion (Landsat 7, Landsat 8, Sentinel-2), produces a more balanced and continuous vegetation classification. The integration highlights vegetation expansion in tidal channels, patchy wetland vegetation, and sabkha

transitions more effectively. The fusion enhances the ability to track geomorphic changes such as colonisation of mudflats by pioneer vegetation, vegetation dieback due to salinity shifts, or sediment deposition influencing vegetation distribution.

The key insight from these analyses for geomorphic change detection shows that Landsat alone provides coarse but reliable long-term monitoring of vegetation changes, while Sentinel-2 detects finer-scale vegetation and geomorphic transitions in coastal environments. The Fusion of Landsat and Sentinel-2, combined with SAR and machine learning, strengthens the detection of vegetation-related geomorphic processes, such as tidal creek development, sediment redistribution, and the spread of halophytic vegetation in sabkha environments. This integrated approach provides a more accurate and resilient monitoring framework for assessing ecological and geomorphic changes in hyper-arid coastal systems like Khor Al-Sabiyeh.

The NDVI results for Khor Al-Sabiyeh highlight significant differences in vegetation detection among the individual satellite sensors and the fused product. Landsat 7 and Landsat 8 outputs were dominated by low NDVI values, largely reflecting the prevalence of bare soil, sabkhas, and tidal flats characteristic of arid coastal systems in Kuwait. Although both sensors delineated water bodies and barren surfaces effectively, they underrepresented small patches of vegetation, which are crucial indicators of geomorphic and ecological change. By contrast, Sentinel-2 imagery, with its higher spatial and spectral resolution, more effectively identified localised vegetation growth along tidal channels and wetland zones. This improved capacity for vegetation detection supports earlier findings that Sentinel-2 enhances the monitoring of vegetation health and distribution in coastal and arid environments (Mandanici & Bitelli, 2016; Delegido et al., 2011).

The fused NDVI product, integrating Landsat 7, Landsat 8, and Sentinel-2, provided the most comprehensive representation of vegetation and geomorphic features, capturing both the broad-scale temporal consistency of Landsat and the fine-scale spatial detail of Sentinel-2. The enhanced delineation of tidal creeks, salt marshes, and vegetation encroachment zones demonstrates the value of multi-sensor fusion for detecting subtle geomorphic processes, including sediment deposition, vegetation succession, and salinity-driven vegetation dieback. These findings align with recent studies emphasising the potential of data fusion, particularly when combined with SAR and machine learning, to strengthen

coastal change detection and environmental monitoring (Müller et al., 2020; Zhang et al., 2021). In the context of Khor Al-Sabiyeh, such approaches provide critical insights into the dynamic interplay between vegetation and geomorphic processes, enabling more effective management of vulnerable coastal ecosystems under the pressures of climate variability and human activity.

(b) NDMI:

The Normalised Difference Moisture Index (NDMI) is an index used to assess the water content in vegetation and the moisture status of ecosystems. It is calculated using reflectance measurements in the near-infrared (NIR) and shortwave infrared (SWIR) bands. The NDMI values range in Figure 4 of -1 to -0.5 indicate very low moisture content, indicating very dry conditions in vegetation; -0.5 to 0: Low moisture content, representing dry to moderately dry conditions; 0 to 0.3: Moderate moisture content, suggesting that vegetation has a reasonable level of water; and 0.3 to 1: High moisture content, indicating lush, water-rich vegetation. Here, the Lower Values (that is, negative values or values close to zero) usually indicate that vegetation is stressed due to a lack of water. This can be due to drought conditions, disease, or other factors that cause vegetation to have less water content, while the Higher Values (that is, Higher NDMI values) signify that vegetation is healthy and has a sufficient or high water content. This is typical of areas with abundant rainfall or well-irrigated agricultural land. NDMI is particularly useful for monitoring droughts, assessing crop health, and managing water resources in forestry and agriculture. By comparing NDMI values over time, researchers and resource managers can detect changes in vegetation moisture levels, which is critical for early drought warning systems and other environmental management applications.

NDMI values indicate surface moisture conditions, ranging from -1 (very dry/built-up/bare soil) to +1 (high vegetation/water moisture). Figure 4 presents four NDMI outputs for 2023 using different datasets: (a) Landsat 8; (b) Landsat 7; (c) Sentinel-2; and, (d) Fusion of Landsat 7, Landsat 8, and Sentinel-2. The focus is to assess how combining SAR, optical, and machine learning techniques enhances geomorphic change detection in the coastal environment.

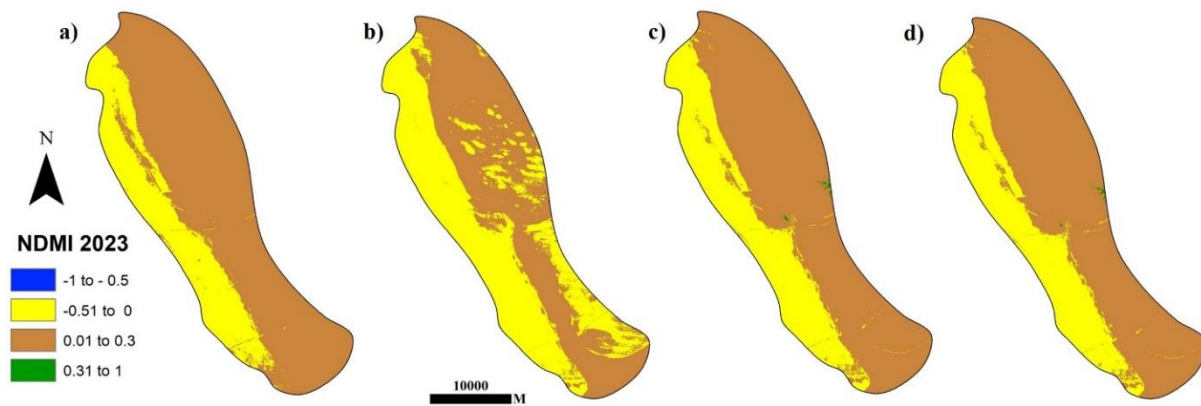


Figure 4: The NDMI for Khor Al-Sabiyeh, Kuwait (a) Landsat 8, Landsat 7 (b) Sentinel 2 (c) and the fusion of the three images (d).

The analyses of NDMI as presented for Figure 4 (a), Landsat 8, show a dominant distribution of yellow (-0.51 to 0) and brown (-1 to -0.5) zones, indicating large areas of dry bare soil and low-moisture surfaces, typical of Kuwait's arid coastal flats; Limited patches of higher NDMI values (green, 0.01–0.3) suggest sparse vegetation or wetter sediments. Figure 4 (b), Landsat 7, similarly indicates a general pattern, but with more scattered green patches compared to Landsat 8. This suggests Landsat 7 detects slightly more moisture variability, possibly due to differences in sensor calibration or temporal acquisition. Coastal and inland geomorphic features are better distinguished compared to (a). Figure 4 (c) shows NDMI analysis for Sentinel-2. The output highlights smaller patches of positive NDMI (green zones) more clearly, indicating improved detection of moisture in salt marshes, tidal flats, and vegetated areas.

This allows for better identification of geomorphic changes, such as shifts in wetland boundaries or vegetation expansion. Figure 4 (d), Fusion (Landsat 7, Landsat 8, Sentinel-2), NDMI analyses produce a more balanced and refined classification. The integration enhances the continuity of moisture-related features, minimising sensor-specific noise. Coastal geomorphic zones—like mudflats, sabkhas (salt flats), and vegetated patches—are more distinctly separated. This (Figure 4d output) demonstrates how fusion + machine learning can capture subtle geomorphic changes, such as tidal creek expansion, sediment deposition, or vegetation encroachment.

The key insights from these NDMI analyses for geomorphic change detection shows that Landsat alone provides a general view but lacks sensitivity to subtle variations; Sentinel-2 improves detection of small-scale geomorphic features due to finer resolution while Fusion of

Landsat and Sentinel-2 integrates both broad-scale temporal coverage (Landsat) and high-resolution spatial detail (Sentinel-2), enhancing the capacity to detect geomorphic changes in the Khor Al-Sabiyeh coastal environment. When coupled with SAR (sensitive to surface roughness and inundation) and machine learning, this fusion approach provides a robust system for monitoring moisture-driven geomorphic dynamics in Kuwait's vulnerable coastal zone.

The NDMI outputs derived from Landsat 7, Landsat 8, and Sentinel-2 imagery illustrate the spatial variability of surface moisture and geomorphic features in Khor Al-Sabiyeh. Landsat imagery provides broad coverage and highlights the dominance of low-moisture classes, consistent with the arid coastal environment of Kuwait, but it underrepresents localised geomorphic variability. Sentinel-2, by contrast, captures finer-scale heterogeneity in tidal flats and vegetated patches due to its higher spatial and spectral resolution, which has been shown to improve vegetation and soil moisture mapping in coastal ecosystems (Houborg et al., 2015; Mandanici & Bitelli, 2016). The presence of scattered positive NDMI values in Sentinel-2 outputs reveals subtle geomorphic processes, such as vegetation encroachment into mudflats and moisture retention in sabkhas, that may be overlooked in coarser-resolution Landsat products.

The fused dataset, integrating Landsat and Sentinel-2, demonstrates superior capability for geomorphic change detection by combining the temporal depth of Landsat with the spatial detail of Sentinel-2, producing a more robust characterisation of moisture-related features. This aligns with previous studies emphasising the advantages of multi-sensor fusion for coastal monitoring (Müller et al., 2020; Zhang et al., 2021). The enhanced delineation of tidal creeks, salt marshes, and sediment deposition zones in the fused NDMI map highlights the potential of integrated optical and SAR data, supported by machine learning algorithms, to detect dynamic geomorphic shifts in hyper-arid coastal systems. Such approaches are critical for assessing the impacts of climate variability, sea-level rise, and anthropogenic pressures on the stability of the Khor Al-Sabiyeh coastal environment, providing essential insights for sustainable management and conservation planning.

(c) MNDWI:

The Modified Normalised Difference Water Index (MNDWI) is a remote sensing index used to enhance the detection of open water features while minimising the influence of built-up land and vegetation. It uses reflectance measurements in the green and shortwave infrared (SWIR)

bands. The MNDWI values in Figure 5 indicate three distinct values from the analyses: Negative Values, typically associated with non-water features such as built-up areas, vegetation, or dry soil. These surfaces reflect more in the SWIR band compared to the green band. Zero to Low Positive Values: may indicate shallow water, turbid water, or areas with a mix of water and other features; and, High Positive Values: which represent open water bodies, as water strongly absorbs SWIR light and reflects green light, leading to higher MNDWI values. The Negative Values, values less than zero, suggest the absence of water, often representing urban structures, vegetation, or bare land; and the Positive Values indicate the presence of water. The higher the value, the more likely it is to be a substantial or open-water body. High MNDWI values are particularly useful for identifying clear water or water saturated environment.

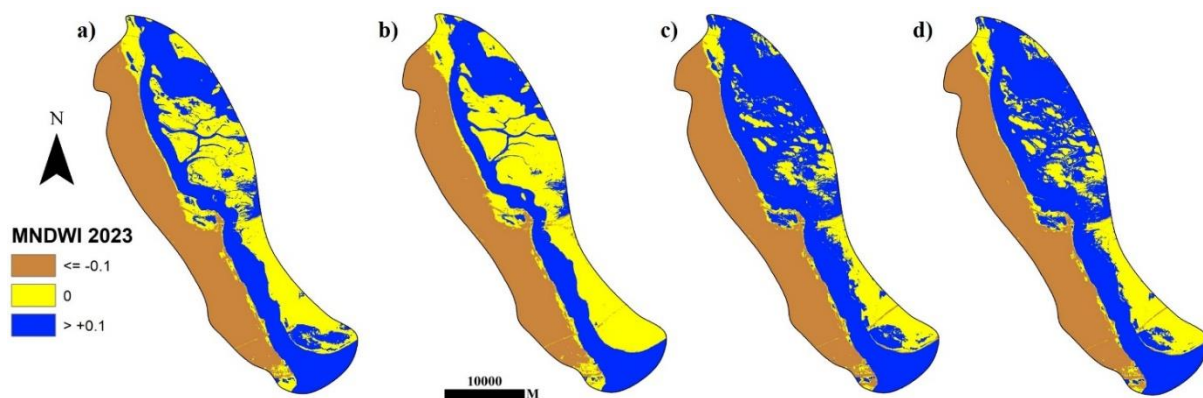


Figure 5: The MNDWI for Khor Al-Sabiyeh, Kuwait (a) Landsat 8, Landsat 7 (b), Sentinel 2 (c) and the fusion of the three images (d).

The Modified Normalised Difference Water Index (MNDWI) results for Khor Al-Sabiyeh in 2023 highlight the spatial distribution of water and land features across different sensors (Figure 5). The classification scheme distinguishes water bodies (blue, >0.1), transitional or mixed zones (yellow, ≈ 0), and non-water features such as bare soil or sediment deposits (brown, ≤ -0.1). The Landsat 8 (Fig. 5a) and Landsat 7 (Fig. 5b) outputs capture major tidal channels and lagoonal waters, but their coarser resolution limits the delineation of narrow intertidal creeks. Sentinel-2 (Fig. 5c), owing to its finer 10 m spatial resolution and higher radiometric sensitivity, provides more detailed mapping of fragmented water patches and smaller tidal features, which are critical for detecting subtle hydrological and geomorphic dynamics (Xu, 2006; Du et al., 2016). The fused image (Fig. 5d) integrates the strengths of

all three sensors, offering enhanced spatial coherence, reduced noise, and improved boundary detection between water and sedimentary flats, thereby overcoming the limitations of individual datasets.

From a geomorphic and ecological monitoring perspective, the MNDWI outputs provide valuable insights into the hydrological regime of Khor Al-Sabiyeh, which is central to its sediment dynamics, tidal flushing, and ecological productivity. Water extent variability captured through MNDWI directly informs assessments of tidal inundation, sediment deposition, and erosion patterns—processes that drive the evolution of coastal wetlands (Ji et al., 2009; Rokni et al., 2014). Moreover, the fusion of optical indices with Synthetic Aperture Radar (SAR) and machine learning enables monitoring of inundation dynamics under varying tidal stages and atmospheric conditions, strengthening the detection of seasonal or episodic changes (Tiner, 2009; White et al., 2020). In the context of Kuwait's rapidly changing coastal systems, such integrated approaches provide a robust framework for early detection of geomorphic transformations and for guiding sustainable wetland management policies in vulnerable regions like Khor Al-Sabiyeh.

(d) SR:

The Simple Ratio (SR) is a remote sensing index used to assess vegetation health and density by comparing the reflectance in the near-infrared (NIR) band to the reflectance in the red band. The SR is calculated as: $SR = NIR / Red$. The SR values greater than 1 typically indicate healthy vegetation. Vegetation strongly absorbs red light for photosynthesis and reflects NIR light. The higher the SR value, the healthier and denser the vegetation, as more NIR is reflected relative to the red light absorbed. The SR values close to 1, however, suggest sparse or less healthy vegetation. In such cases, the reflectance in the red and NIR bands is more balanced, indicating less vigorous plant growth or sparser vegetation cover. Also, the SR values less than 1 are rare and usually indicate non-vegetated surfaces or highly stressed vegetation. Surfaces like water bodies, urban areas, or bare soil often reflect more red light than NIR light.

The SR is a straightforward index that highlights differences in vegetation conditions. It is sensitive to variations in chlorophyll content, making it useful for monitoring plant health, assessing biomass, and evaluating crop conditions. However, like other vegetation indices, it may be affected by factors such as soil background, atmospheric conditions, and sensor noise.

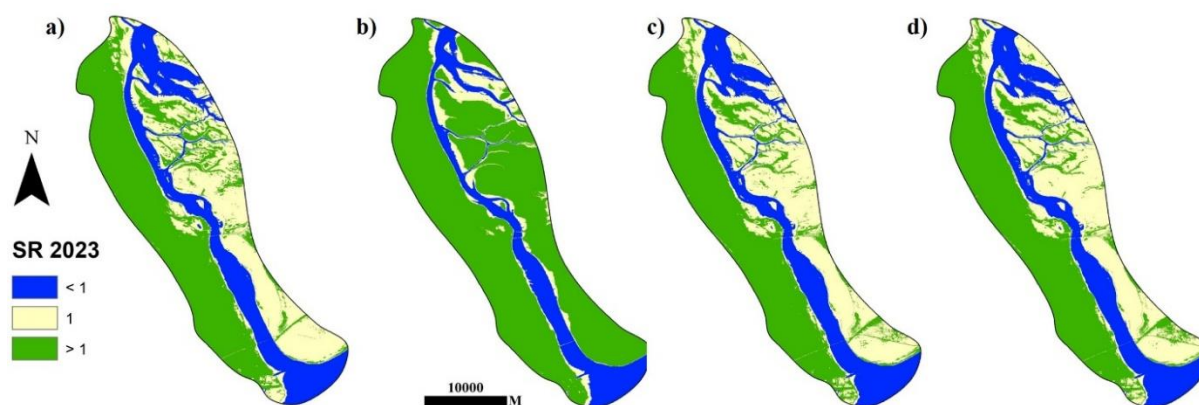


Figure 6: The SR for Khor Al-Sabiyeh, Kuwait (a) Landsat 8, Landsat 7 (b), Sentinel 2 (c) and the fusion of the three images (d).

Figure 6 presents the Simple Ratio (SR) index for Khor Al-Sabiyeh, Kuwait, for the year 2023, derived from (a) Landsat 8, (b) Landsat 7, (c) Sentinel-2, and (d) a fusion of the three datasets. The SR, which is a vegetation index based on the ratio between near-infrared (NIR) and red reflectance, is an established indicator of vegetation vigour and biomass. In this representation, blue values correspond to $SR < 1$ (indicative of water bodies or barren surfaces), cream-colored areas ($SR \approx 1$) reflect transitional zones with sparse or stressed vegetation, and green values ($SR > 1$) correspond to relatively healthier and denser vegetation cover.

Figure 6 (a), from Landsat 8, shows distinct separation of water channels and intertidal zones (blue) from barren and possibly vegetated areas (green), with improved radiometric performance allowing clear delineation of wetland vegetation patches. Figure 6 (b), from Landsat 7, highlights similar patterns but with less clarity due to sensor degradation issues (SLC-off problem), leading to potential data gaps and striping. Figure 6 (c), derived from Sentinel-2, provides enhanced spatial detail, allowing for finer detection of vegetation heterogeneity within tidal flats and salt marsh areas. This is especially important in coastal wetlands like Khor Al-Sabiyeh, where vegetation distribution is patchy and linked to subtle geomorphic and hydrological gradients. Figure 6 (d), representing the fusion of Landsat 7, Landsat 8, and Sentinel-2, illustrates the advantages of multi-sensor integration. The composite imagery minimises data gaps, enhances spatial continuity, and provides a more accurate assessment of vegetation distribution across the coastal wetland. This fusion

approach enhances the reliability of SR for monitoring geomorphic and ecological processes, such as sediment deposition influencing vegetation colonisation, tidal channel shifts, and shoreline stability.

From a geomorphic change detection perspective, SR is particularly valuable in distinguishing between bare sedimentary surfaces, inundated zones, and vegetated landforms. In Khor Al-Sabiyeh, the ability to track vegetation health and expansion or retreat along tidal creeks and mudflats provides indirect evidence of geomorphic processes such as erosion, accretion, and salt marsh succession. By integrating SR with SAR data, which is sensitive to surface roughness and inundation, and machine learning algorithms, which improve classification accuracy, researchers and policy makers can generate robust spatio-temporal models of wetland geomorphic dynamics. This integrated framework thus enhances the detection of geomorphic changes and supports effective coastal management strategies in response to climate change and anthropogenic pressures in Kuwait.

The spatial and temporal variability illustrated in the index outputs highlights the sensitivity of remotely sensed indicators to seasonal and land cover changes. The observed variability also reflects differences in sensor acquisition dates and atmospheric conditions, which may introduce subtle inconsistencies in the continuity of the time series (Roy et al., 2014). Nonetheless, the general patterns align with expected seasonal dynamics, suggesting that the indices reliably capture land surface processes relevant to geomorphic and ecological conditions in the study area (Tucker, 1979; Gao, 1996, 2020). From an applied perspective, these temporal trajectories offer valuable insights for monitoring both short-term disturbances and longer-term environmental change. The capacity to track shifts in vegetation and/or bare surfaces' vigour, surface wetness, or soil exposure makes the indices particularly useful for assessing land degradation, habitat condition, and the impacts of hydrological variability (Forkel et al., 2013; Peña-Arancibia et al., 2017). In arid and semi-arid settings such as Kuwait, where ecosystems are highly responsive to rainfall pulses and anthropogenic pressure, such indicators provide an efficient means to quantify and interpret environmental dynamics. Moreover, the integration of these time-series metrics with ground-based or ancillary data could strengthen their application for land management, early-warning monitoring, and policy-relevant ecological assessments (Zhu et al., 2019).

(e) Band Ratio 54:

The Band Ratio 54, also known as the NIR/SWIR band ratio, is an index commonly used in remote sensing for a variety of applications, including vegetation analysis, water content, and mineral exploration. The High Band Ratio 54 value indicates a strong reflectance in the near-infrared (NIR) band relative to the shortwave infrared (SWIR) band. This is often characteristic of healthy and dense vegetation, which reflects more in the NIR band due to its cellular structure and water content, while absorbing more in the SWIR band. The Moderate values may suggest areas with less dense vegetation, vegetation under some stress, or a mix of vegetation and non-vegetative elements like soil or urban features. The Low Band Ratio 54 values, on the other hand, occur when there is a low reflectance in the NIR band relative to the SWIR band. This can indicate non-vegetated surfaces, such as water bodies, urban areas, or bare soils. In particular, surfaces with high moisture content, like water bodies, tend to reflect less NIR and more SWIR, resulting in lower Band Ratio 54 values.

The Band Ratio 54 is useful in distinguishing between different types of land cover and assessing vegetation health. It can also be valuable in detecting water stress in plants, since vegetation with lower water content will have different NIR and SWIR reflectance properties.

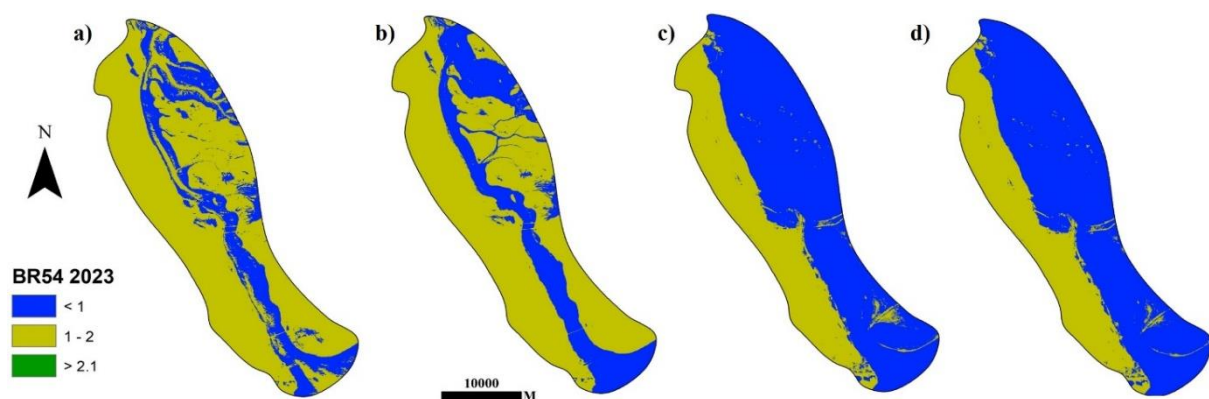


Figure 7: The BR 54 for Khor Al-Sabiyeh, Kuwait (a) Landsat 8, Landsat 7 (b), Sentinel 2 (c) and the fusion of the three images (d).

The Band Ratio 54 (BR54) outputs (Figure 7) for Khor Al-Sabiyeh highlight the spatial variability of geomorphic and ecological features across sensors. In the Landsat 8 (Fig. 7a) and

Landsat 7 (Fig. 7b) maps, the ratio values reveal clear differentiation between water bodies (blue, <1), intertidal and sedimentary flats (yellow, $1-2$), and vegetated or more structurally complex surfaces (green, >2.1). These transitions reflect the sensitivity of the BR54 ratio—commonly derived from shortwave infrared and near-infrared bands—to variations in surface moisture, vegetation presence, and substrate composition. Sentinel-2 (Fig. 7c) did not provide a more refined delineation of tidal channels and small-scale sedimentary features. The fused product (Fig. 7d) integrates the strengths of all three sensors and was expected to produce a more coherent and spatially continuous classification of the coastal landscape. The result of the BR54 fusion analyses did not, however, produce a more robust mapping of geomorphic changes, particularly in the intertidal flats and lagoonal margins, where sediment redistribution and vegetation colonisation are dynamic.

The Band Ratio 54 (BR54) results for Khor Al-Sabiyeh provide valuable insights into the geomorphic variability of this dynamic coastal system. Across the individual datasets—Landsat 8 and Landsat 7—the BR54 index successfully discriminates between aquatic zones (values <1), transitional intertidal and sedimentary flats ($1-2$), and vegetated or structurally complex surfaces (>2.1). These outputs are consistent with previous findings that band ratios utilising shortwave infrared (SWIR) and near-infrared (NIR) wavelengths enhance the sensitivity of optical imagery to moisture content, vegetation density, and sediment characteristics (Jensen, 2007; Roy et al., 2014).

In Khor Al-Sabiyeh, where tidal flows, sediment transport, and ecological succession interact, such integrative approaches are essential for capturing both gradual and episodic changes. The fused BR54 outputs, enhanced by SAR and machine learning, therefore provide a powerful framework for advancing coastal geomorphic monitoring and informing sustainable management of Kuwait's vulnerable coastal ecosystems.

(f) Band Ratio 35:

The Band Ratio 35 typically refers to the ratio of reflectance values in specific spectral bands used in remote sensing, where "3" and "5" correspond to particular wavelengths on a multispectral sensor. The exact bands these numbers refer to can vary depending on the satellite or sensor being used. However, a common interpretation of Band Ratio 35, when used in certain sensors like Landsat, refers to the ratio of the red band (Band 3) to the near-infrared band (Band

5). High Band Ratio 35 values indicate that the reflectance in the red band is significantly higher relative to the near-infrared band. This is usually indicative of non-vegetated surfaces such as bare soil, urban areas, or water bodies. It may also suggest stressed or unhealthy vegetation that reflects more red light. Moderate values suggest a balance between the red and near-infrared reflectance. This could be characteristic of areas with sparse vegetation or transitional areas where there is a mix of vegetation and non-vegetated surfaces. Low Band Ratio 35 values indicate higher reflectance in the near-infrared band relative to the red band. This is typical of healthy and dense vegetation, which absorbs red light for photosynthesis and reflects a lot of near-infrared light.

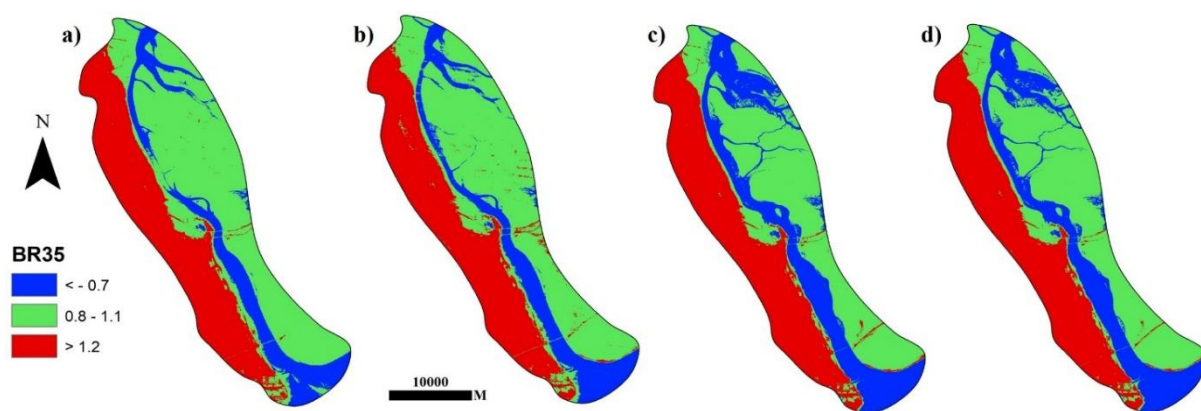


Figure 8: The BR 35 for Khor Al-Sabiyeh, Kuwait (a) Landsat 8, Landsat 7 (b), Sentinel 2 (c) and the fusion of the three images (d).

The Band Ratio 3/5 (BR35) imagery for Khor Al-Sabiyeh in 2023 highlights the spatial distribution of geomorphic surfaces and provides insights into vegetation, soil, and water discrimination (Figure 8). BR35 typically enhances the contrast between vegetated and non-vegetated areas by exploiting the reflectance properties of the red (band 3) and shortwave infrared (band 5) wavelengths (Jensen, 2015). In the Landsat 8 (Fig 8a) and Landsat 7 (Fig. 8b) outputs, large sections of the lagoon margin and intertidal flats are mapped in red (>1.2), representing dry or saline surfaces with high SWIR reflectance, while vegetated and moist zones appear in green ($0.8-1.1$), and open water or saturated zones are captured in blue (<-0.7). The Sentinel-2 image (Fig. 8c), benefiting from finer spatial and radiometric resolution, delineates smaller-scale features such as tidal creeks and transitional mudflat-vegetation boundaries more effectively than the Landsat sensors. The fused image (Fig. 8d) integrates these datasets, reducing noise and providing greater consistency in geomorphic unit

detection.

From an ecological and geomorphic monitoring perspective, BR35 proves particularly useful for detecting salinity-driven changes, shoreline erosion, and vegetation stress, which are critical processes shaping the dynamics of Khor Al-Sabiyeh. The red-dominated areas suggest expansion of saline and bare mudflat zones, while the green and blue categories highlight areas that retain ecological productivity and hydrological connectivity. By integrating BR35 with other indices (NDVI, NDMI, and MNDWI) and incorporating SAR data, machine learning models can more accurately map and monitor subtle geomorphic transformations, particularly in transitional intertidal zones (Adam et al., 2010; White et al., 2020). This integration enhances the ability to track long-term wetland stability, inform conservation interventions, and evaluate the implications of climate change and anthropogenic pressures on Kuwait's vulnerable coastal ecosystems.

Conclusion and Recommendation

The comparative analysis of Landsat 7, Landsat 8, Sentinel-2, and their fused datasets highlights the differential capacity of each sensor to capture geomorphic variability in the Khor Al-Sabiyeh coastal environment. While Landsat 7 and Landsat 8 provide valuable long-term continuity and moderate spatial resolution suitable for trend detection, Sentinel-2 imagery offers higher spatial and spectral fidelity that improves the delineation of subtle geomorphic features. The fusion of the three datasets further enhances interpretative power by combining the temporal depth of Landsat with the spatial precision of Sentinel-2, resulting in improved accuracy in the detection of shoreline shifts, sediment redistribution, and vegetation dynamics.

Based on these results, the integration of fused optical datasets with SAR and machine learning algorithms is recommended as the most suitable approach for enhanced detection of geomorphic changes in Khor Al-Sabiyeh. The fusion process maximises data richness and minimizes sensor-specific limitations, while SAR contributes complementary information on surface texture and inundation dynamics. Future studies should prioritize hybrid fusion and classification frameworks that leverage machine learning to assimilate multi-sensor inputs, thereby offering a robust, scalable methodology for coastal monitoring and management in dynamic environments such as the northern Arabian Gulf.

Acknowledgements

This work was supported and funded by the Kuwait University Research Grant No. R001/22. A.E.A. and T.D.T.O. appreciate Kuwait University for the grant provided for this ongoing work.

References

- Adam, E., Mutanga, O., & Rugege, D. (2010). Multispectral and hyperspectral remote sensing for identification and mapping of wetland vegetation: A review. *Wetlands Ecology and Management*, 18 (3), 281-296.
- Al-Attar, M., Al-Sudairawi, M., Al-Hurban, A., & Al-Dousari, A. (2023). Coastal vulnerability and geomorphological change assessment of the Kuwait shoreline. *Journal of Coastal Conservation*, 27 (1), 12. <https://doi.org/10.1007/s11852-023-00952-3>
- Al-Hurban, A., Al-Sarawi, M., & Massoud, M. (2008). Environmental impact of coastal dredging and land reclamation on the sediment quality of Kuwait Bay. *Environmental Geology*, 53 (2), 401–414. <https://doi.org/10.1007/s00254-007-0640-4>
- Al-Rashed, M., Kwarteng, A. Y., & Khan, N. (2017). Monitoring wetland environmental changes in the Kuwaiti coastal area using remote sensing. *Journal of Coastal Conservation*, 21 (3), 279-292.
- Ban, Y., Zhang, P., Nascetti, A., Bevington, A. R., & Wulder, M. A. (2015). Near real-time flood mapping using satellite SAR data: A review. *Remote Sensing*, 7(12), 14602–14623. <https://doi.org/10.3390/rs71114602>.
- Belgiu, M., & Drăguț, L. (2016). Random forest in remote sensing: A review of applications and future directions. *ISPRS Journal of Photogrammetry and Remote Sensing*, 114, 24–31. <https://doi.org/10.1016/j.isprsjprs.2016.01>.
- Chen, C., Davis, C., & Warnken, M. (2005). Improved procedures for the estimation of water surface evaporation from thermally stratified reservoirs. *Journal of Hydrology*, 308(1-4), 412-424.
- Delegido, J., Verrelst, J., Alonso, L., & Moreno, J. (2011). Evaluation of Sentinel-2 red-edge bands for empirical estimation of green LAI and chlorophyll content. *Sensors*, 11(7), 7063–7081. <https://doi.org/10.3390/s110707063>.
- Drusch, M., Del Bello, U., Carlier, S., Colin, O., Fernandez, V., Gascon, F., Hoersch, B., Isola, C., Laberinti, P., Martimort, P., Meygret, A., Spoto, F., Sy, O., Marchese, F., & Bargellini, P. (2012). Sentinel-2: ESA's optical high-resolution mission for GMES operational services. *Remote Sensing of Environment*, 120, 25–36. <https://doi.org/10.1016/j.rse.2011.11.026>
- Du, Y., Zhang, Y., Ling, F., Wang, Q., Li, W., & Li, X. (2016). Water bodies mapping from Sentinel-2 imagery with Modified Normalized Difference Water Index at 10-m spatial resolution produced by sharpening the SWIR band. *Remote Sensing*, 8(4), 354. <https://doi.org/10.3390/rs8040354>.

- European Space Agency. (2023). Mission Status Report 201: Sentinel-2 (October 2023). ESA
- Forkel, M., Carvalhais, N., Verbesselt, J., Mahecha, M. D., Neigh, C. S., & Reichstein, M. (2013). Trend change detection in NDVI time series: Effects of inter-annual variability and methodology. *Remote Sensing*, 5(5), 2113–2144. <https://doi.org/10.3390/rs5052113>.
- Gao, B. C. (1996). NDWI—A normalized difference water index for remote sensing of vegetation liquid water from space. *Remote Sensing of Environment*, 58(3), 257–266. <https://doi.org/10.1016/S0034-4257%2896%2900067-3>.
- Gao, B., Shen, H., & Wang, Y. (2020). Application of Sentinel-2 data for wetland monitoring and assessment. *Remote Sensing*, 12(15), 2456. <https://doi.org/10.3390/rs12152456>
- Goodfellow, I., Bengio, Y., & Courville, A. (2016). *Deep learning*. MIT Press.
- Giri, C., Ochieng, E., Tieszen, L. L., Zhu, Z., Singh, A., Loveland, T., ... & Duke, N. (2011). Status and distribution of mangrove forests of the world using earth observation satellite data. *Global Ecology and Biogeography*, 20(1), 154-159.
- Goodfellow, I., Bengio, Y., & Courville, A. (2016). *Deep learning*. MIT Press.
- Houborg, R., McCabe, M. F., Cescatti, A., Gao, F., Schull, M. A., & Gitelson, A. A. (2015). Joint leaf chlorophyll content and leaf area index retrieval from Landsat data using a regularized model inversion system (REGFLEC). *Remote Sensing of Environment*, 159, 203–221. <https://doi.org/10.1016/j.rse.2014.12.008>.
- Irons, J. R., Dwyer, J. L., & Barsi, J. A. (2012). The next Landsat satellite: The Landsat Data Continuity Mission. *Remote Sensing of Environment*, 122, 11–21. <https://doi.org/10.1016/j.rse.2011.08.026>.
- Jensen, J. R. (2007). *Remote sensing of the environment: An Earth resource perspective* (2nd ed.). Pearson Prentice Hall.
- Jensen, J. R. (2015). *Introductory digital image processing: A remote sensing perspective* (4th ed.). Pearson.
- Ji, L., Zhang, L., & Wylie, B. (2009). Analysis of dynamic thresholds for the Normalised Difference Water Index. *Photogrammetric Engineering & Remote Sensing*, 75(11), 1307–1317. <https://doi.org/10.14358/PERS.75.11.1307>
- Jordan, C. F. (1969). Derivation of leaf-area index from quality of light on the forest floor. *Ecology*, 50(4), 663-666.
- Kuenzer, C., Bluemel, A., Gebhardt, S., Quoc, T. V., & Dech, S. (2011). Remote sensing of mangrove ecosystems: A review. *Remote Sensing*, 3(5), 878-928.
- Ma, L., Li, M., Ma, X., Du, P., & Liu, Y. (2019). Deep learning in remote sensing applications: A meta-analysis and review. *ISPRS Journal of Photogrammetry and Remote Sensing*, 152, 166–177. <https://doi.org/10.1016/j.isprsjprs.2019.04.022>

- Mandanici, E., & Bitelli, G. (2016). Preliminary comparison of Sentinel-2 and Landsat 8 imagery for a combined use. *Remote Sensing*, 8(12), 1014. <https://doi.org/10.3390/rs8121014>.
- Mitsch, W. J., & Gosselink, J. G. (2015). *Wetlands* (5th ed.). John Wiley & Sons.
- Müller, M., Schneider, M., & Gunther, A. (2016). The application of remote sensing for the detection of coastal geomorphological changes. *Remote Sensing*, 8(12), 955.
- Murray, N.J., Phinn, S.R., DeWitt, M. et al. The global distribution and trajectory of tidal flats. *Nature* 565, 222–225 (2019). <https://doi.org/10.1038/s41586-018-0805-8>
- Nicholls, R. J., & Cazenave, A. (2010). Sea-Level Rise and Its Impact on Coastal Zones. *Science*, 328(5985), 1517–1520. DOI: 10.1126/science.1185782.
- Peña-Arancibia, J. L., McVicar, T. R., Paydar, Z., Li, L. T., Guerschman, J. P., Donohue, R. J., ... & Chiew, F. H. S. (2017). Dynamic identification of summer cropping irrigated areas in a large region using MODIS time series and random forests. *Remote Sensing of Environment*, 190, 318–330. (<https://doi.org/10.1016/j.rse.2016.12.020>)
- Rokni, K., Ahmad, A., Selamat, A., & Hazini, S. (2014). Water feature extraction and change detection using multitemporal Landsat imagery. *Remote Sensing*, 6(5), 4173–4189. <https://doi.org/10.3390/rs6054173>.
- Rouse, J. W., Haas, R. H., Schell, J. A., & Deering, D. W. (1974). Monitoring vegetation systems in the Great Plains with ERTS. *Proceedings of the Third Earth Resources Technology Satellite-1 Symposium*, 1, 309-317
- Roy, D. P., Wulder, M. A., Loveland, T. R., Woodcock, C. E., Allen, R. G., Anderson, M. C., Helder, D., Irons, J. R., Johnson, D. M., Kennedy, R., Scambos, T. A., Schaaf, C. B., Schott, J. R., Sheng, Y., Vermote, E. F., Belward, A. S., Bindschadler, R., Cohen, W. B., Gao, F., ... Zhu, Z. (2014). Landsat-8: Science and product vision for terrestrial global change research. *Remote Sensing of Environment*, 145, 154–172. <https://doi.org/10.1016/j.rse.2014.02.001>.
- Sabins, F. F. (1996). *Remote sensing: principles and interpretation* (3rd ed.). W.H. Freeman and Co.
- Tiner, R. W. (2009). *Wetland indicators: A guide to wetland identification, delineation, classification, and mapping*. CRC Press.
- United States Geological Survey (USGS). (2003). SLC-off gap-filled products: Gap-filled SLC-off Landsat ETM+ data products generated by the USGS EROS Data Center. U.S. Geological Survey. Retrieved from <https://landsat.usgs.gov/slc>
- U.S. Geological Survey. (2023). *Landsat missions: Imaging the Earth since 1972*. U.S. Geological Survey. <https://www.usgs.gov/landsat-missions>
- White, L., Brisco, B., Pregitzer, M., Tedford, B., & Boychuk, L. (2020). Wetland habitat monitoring using multi-sensor remote sensing. *Remote Sensing*, 12(4), 591. <https://doi.org/10.3390/rs12040591>

Xu, H. (2006). Modification of normalized difference water index (NDWI) to enhance open water features in remotely sensed imagery. *International Journal of Remote Sensing*, 27(14), 3025–3033. <https://doi.org/10.1080/01431160600589179>.

Zhang, Q., Li, H., & Wu, B. (2021). Machine learning-based integrated assessment of ecosystem vulnerability using remote sensing data. *Environmental Modelling & Software*, 137, 104948. <https://doi.org/10.1016/j.envsoft.2020.104948>

Zhu, Z., Woodcock, C. E., Holden, C., & Yang, Z. (2019). Generating synthetic Landsat images based on all available Landsat data: Predicting Landsat surface reflectance at any given time. *Remote Sensing of Environment*, 231, 111204. <https://doi.org/10.1016/j.rse.2019.111204>.